

## Semisynthesis and *in vitro* anticancer activities of andrographolide analogues

Srinivasa Rao Jada<sup>a</sup>, Genevieve Suseno Subur<sup>b</sup>, Charlie Matthews<sup>c</sup>,  
Ahmad Sazali Hamzah<sup>d</sup>, Nordin Haji Lajis<sup>e</sup>, Mohammad Said Saad<sup>f</sup>,  
Malcolm F.G. Stevens<sup>c</sup>, Johnson Stanslas<sup>a,c,\*</sup>

<sup>a</sup> Faculty of Medicine and Health Sciences, Universiti Putra Malaysia, 43400 Serdang, Selangor, Malaysia

<sup>b</sup> The School of Pharmacy, University of London, 29/39 Brunswick Square, WC1N 1AX London, United Kingdom

<sup>c</sup> Centre for Biomolecular Sciences, School of Pharmacy, University of Nottingham, NG7 2RD Nottingham, United Kingdom

<sup>d</sup> Institute of Science, Universiti Teknologi MARA, 40450 Shah Alam, Malaysia

<sup>e</sup> Institute of Bioscience, Universiti Putra Malaysia, 43400 Serdang, Selangor, Malaysia

<sup>f</sup> Faculty of Agriculture, Universiti Putra Malaysia, 43400 Serdang, Selangor, Malaysia

Received 16 January 2006; received in revised form 9 July 2006

Available online 17 January 2007

### Abstract

The plant *Andrographis paniculata* found throughout Southeast Asia contains Andrographolide **1**, a diterpenoid lactone, which has antitumour activities against *in vitro* and *in vivo* breast cancer models. In the present study, we report on the synthesis of andrographolide derivatives, 3,19-isopropylideneandrographolide (**2**), 14-acetyl-3,19-isopropylideneandrographolide (**3**) and 14-acetyl-3,19-isopropylideneandrographolide (**4**), and their *in vitro* antitumour activities against a 2-cell line panel consisting of MCF-7 (breast cancer cell line) and HCT-116 (colon cancer cell line). Compounds **2** and **4** were also screened at the US National Cancer Institute (NCI) for their activities against a panel of 60 human cancer cell lines derived from nine cancer types. Compound **2** was found to be selective towards leukaemia and colon cancer cells, and compound **4** was selective towards leukaemia, ovarian and renal cancer cells at all the dose-response parameters. Compounds **2** and **4** showed non-specific phase of the cell cycle arrest in MCF-7 cells treated at different intervals with different concentrations. NCI's COMPARE and SOM mechanistic analyses indicated that the anticancer activities of these new class of compounds were not similar to that of standard anticancer agents, suggesting novel mechanism(s) of action.

© 2006 Elsevier Ltd. All rights reserved.

**Keywords:** *Andrographis paniculata*; Acanthaceae; Andrographolide; Semisynthesis; Anticancer; Cell cycle

### 1. Introduction

*Andrographis paniculata* Nees (Acanthaceae) is a herb commonly used in India, China and Southeast Asia for the treatment of a large variety of illnesses, which include meningitis, acute hepatitis, and many other acute inflammatory conditions (Chopra et al., 1956; Chang and But, 1987). The main components of *A. paniculata* are the diterpene lactones, of which andrographolide **1** (Fig. 1) is the major one; it is chemically designated as 3-{2-[decahydro-6-hydroxy-5-(hydroxymethyl)-5,8a-dimethyl-2-methylene-1-naphthalenyl]-ethylidene} dihydro-4-hydroxy-2(3H)-furanone.

**Abbreviations:** SAR, structure–activity relationship; CDK, cyclin-dependent kinase; NCI, National Cancer Institute; PBS, phosphate-buffered saline; MTT, 3-[4,5-dimethylthiazol-2-yl]-2,5-diphenyltetrazolium bromide; PI, propidium iodide; DMSO, dimethyl sulfoxide; SOM, self-organising maps; TLC, thin layer chromatography; RPMI 1640, Roswell Park Memorial Institute; FACS, fluorescence-activated cell sorter; CNS, central nervous system; NSCLC, non-small cell lung cancer.

\* Corresponding author. Tel.: +60 3 89472310; fax: +60 3 89436178.

E-mail address: [rcxjs@medic.upm.edu.my](mailto:rcxjs@medic.upm.edu.my) (J. Stanslas).

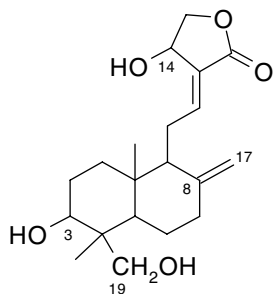


Fig. 1. Chemical structure of andrographolide **1**.

Andrographolide **1** is found in the whole plant but is most concentrated in the leaves. It is a diterpene containing a  $\gamma$ -lactone ring connected to a decalin ring system *via* an unsaturated C-2 moiety (Kleipool, 1952); it has multiple pharmacological activities such as protozoacidal, antihepatotoxic, anti-HIV, immunostimulative, anticancer, hypoglycemic and hypotensive activities (Handa and Sharma, 1990; Siripong et al., 1992; Kapil et al., 1993; Visen et al., 1993; Puri et al., 1993; Matsuda et al., 1994; Basak et al., 1999; Amroyan et al., 1999; Zhang and Tan, 2000; Stanslas et al., 2001; Rajagopal et al., 2003; Srinivasa et al., 2006b). We have previously reported the antitumour potential of andrographolide **1** in *in vivo* breast cancer models (Stanslas et al., 2001), whose anticancer activity is thought to be exerted through blockage of cell cycle progression by the induction of cyclin-dependent kinase inhibitors (CDKI) and with a concomitant decrease in cyclin-dependent kinase (CDK4) expression (Rajagopal et al., 2003). Recent studies suggested that andrographolide **1** is an interesting pharmacophore with anticancer and immunomodulatory activities and hence has the potential to be developed as an anticancer chemotherapeutic agent (Rajagopal et al., 2003; Srinivasa et al., 2006b).

Since andrographolide **1** can be readily isolated in high yield and has antitumour effects against breast cancer models (Stanslas et al., 2001), it was utilised as one of the starting materials for synthesis of derivatives. In the present study, we report the semisynthesis of andrographolide derivatives, their *in vitro* anticancer activities, probable mechanism(s) of action and effects of these compounds on cell cycle progression.

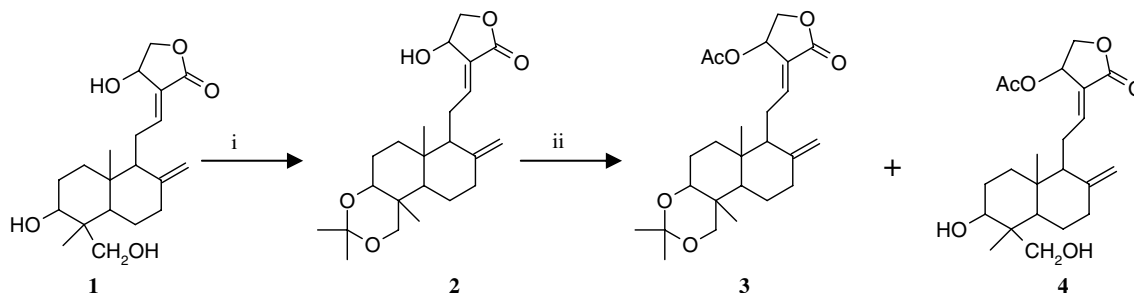
## 2. Results and discussion

### 2.1. Chemistry

Andrographolide **1** is a bicyclic diterpenoid lactone and contains three hydroxyl groups at C-3, C-19 and C-14, these being secondary, primary and allylic, respectively. In a previous report, it has been shown that the intact  $\gamma$ -butyrolactone ring, the double bonds at C-12 and C-13, C-8 and C-17, and C-14 hydroxyl group are responsible for the cytotoxic activity (Nanduri et al., 2004). Since the hydroxyl groups may form hydrogen bonds to biological receptors, a logical first step was to block one or more of them. Starting from a derivative with the exocyclic C-8 and C-17 double bond converted to an epoxide, the propionylation or acetylation of the OH group on the furanone ring maintained, or slightly improved, the antitumour activity, whereas mono-acetylation on a different OH group reduced this activity. On the other hand, acetylation of all three OH groups resulted in an increased antitumour activity (Nanduri et al., 2004; Satyanarayana et al., 2004). The cytotoxic activities of the andrographolide analogues were similar irrespective of the number of carbons of the added groups at C-14 (Nanduri et al., 2004).

The synthetic pathways used in the present work are outlined in Scheme 1 and all employed andrographolide **1** as one of the starting materials. The product of the reaction of andrographolide **1** with 2,2-dimethoxypropane in benzene/DMSO was 3,19-isopropylideneandrographolide (**2**). Acetylation of compound **2** with acetic anhydride yielded 14-acetyl-3,19-isopropylideneandrographolide (**3**) and an unexpected compound 14-acetyl-3,19-isopropylideneandrographolide (**4**). The structures of compounds **2–4** were confirmed by IR,  $^1\text{H}$  NMR,  $^{13}\text{C}$  NMR and mass spectroscopic analyses.

The stereochemistry of andrographolide **1** has previously been established. The two central six-membered rings adopt a chair conformation and the furan ring adopts an envelope conformation (Smith et al., 1982; Fujita et al., 1984; Spek et al., 1987). The structure of compound **4** was confirmed by X-ray crystallography and the atom-numbering scheme matches that used for andrographolide **1** (Spek et al., 1987; Srinivasa et al., 2006a). Andrographolide **1** forms hydrogen-bonded chains at both ends of the



Scheme 1. Synthesis of andrographolide derivatives **2**, **3** and **4**. Reagents and conditions: (i) 2,2-dimethoxypropane, benzene/DMSO, reflux/30 min; (ii) acetic anhydride, reflux/45 min.

molecule, and acetylation of the hydroxyfuranone moiety completely abolished the donation of O–H...O hydrogen bond in that position; acetylation has limited effect on bond distances (Spek et al., 1987; Srinivasa et al., 2006a).

## 2.2. Screening for *in vitro* anticancer activity

The compounds **2–4** were first evaluated for anticancer activity in MCF-7 human breast cancer and HCT-116 colon cancer cell lines. A 72 h MTT cell viability assay (Mosmann, 1983) was performed to determine the growth inhibition and cytotoxic properties of the compounds. The MTT test is a colorimetric assay that measures the percentage of cell survival compared to untreated controls. Cells were treated with at least four different concentrations of compounds ranging from 0.1 to 100  $\mu$ M and three dose-response parameters were calculated: GI<sub>50</sub> (concentration that produces 50% growth inhibition), TGI (concentration that produces total growth inhibition or cytostatic effect) and LC<sub>50</sub> (concentration that produces –50% growth: lethal concentration or “net cell killing” or cytotoxicity parameter) (Boyd and Paull, 1995). Compounds **2** and **4** were equally potent and compound **3** was less potent compared to that of the parent compound in inhibiting the growth of two cell lines based on GI<sub>50</sub> values (Table 1). However, compound **4** was more potent in causing cytostatic (TGI values) effect in MCF-7 cell line compared to that of the parent compound.

The discovery of novel compounds with selectivity patterns is one of the intentions of the screening program. Screening of compounds against the NCI human cancer cell line panel gives a wealth of information on the growth inhibitory effects of molecules across a wide variety of human tumour cell lines including cell type specific effects (selective growth inhibition or cytotoxic properties), correlation with specific genes or protein expression levels, and comparison of the mode of action with molecules of ‘known’ action by COMPARE (computerised pattern-recognition algorithm) analysis (Weinstein et al., 1997). In the NCI screen, 60 human cancer cell lines were treated for 48 h with 10-fold dilutions of compounds at a minimum of five concentrations (0.01–100  $\mu$ M). Sulforhodamine B (SRB) endpoint assay was used to calculate three dose-response parameters: GI<sub>50</sub>, TGI and LC<sub>50</sub> values (Tables 2 and 3) (Monks et al., 1991). Further, a mean graph midpoint (MG\_MID) was calculated for each of the mentioned

parameters, giving an averaged activity parameter over all the cell lines. For the calculation of MG\_MID, insensitive cell lines were included with the highest concentration tested.

Fig. 2 and Table 2 demonstrate that compound **2** was effective against leukaemia (CCRF-CEM, K-562, MOLT-4, RPMI-8226, SR), NSCLC (NCI-H226), colon (HCT-116, SW-620), melanoma (LOX IMVI), ovarian (OVCAR-3, OVCAR-8) and breast (MCF-7, NCI/ADR-RES) cancer cell lines with GI<sub>50</sub> less than 5  $\mu$ M. Compound **4** was effective against leukaemia (CCRF-CEM, K-562, MOLT-4, RPMI-8226, SR), NSCLC (HOP-62, NCI-H226, NCI-H522), colon (HCT-116, HCT-15, SW-620), CNS (SF-539), melanoma (LOX IMVI, UACC-62), ovarian (IGROVI, OVCAR-3), renal (ACHN, SN12C) and breast (MDA-MB-435) cancer cell lines with GI<sub>50</sub> less than 5  $\mu$ M. By averaging the three parameters of dose-response activities (GI<sub>50</sub>, TGI and LC<sub>50</sub>) from the NCI screen (Table 3), compound **4** was the most potent followed by compound **2** and andrographolide **1**, indicating that modifications to andrographolide **1** skeleton improves antitumour activity.

COMPARE analysis of compounds **2** and **4** (Table 4) did not show any discrete mechanism of action of category. In self-organising maps (SOM) analyses, andrographolide **1** and compound **2** were projected in the ‘Q’ region, a region assigned without a known mechanism of action category (Fig. 3). Therefore, SOM analyses suggesting that andrographolide **1** and compound **2** may possess novel mechanism(s) of action. However, compound **4** was projected in the sub-region P<sub>11</sub>, suggesting a possible mode of action that targets phosphatases or kinases involved in cell cycle regulation. This probability is supported by COMPARE analysis, which revealed that the activity of compound **4** is similar to flavopiridol (PCC = 0.562), a kinase inhibitor (Senderowicz et al., 1998).

## 2.3. Determination of cell cycle perturbations by compounds **2** and **4** by flow cytometry

In order to evaluate the cell cycle phase distribution of MCF-7 cells that was restricted by two different concentrations of compounds **2** and **4**, we conducted DNA flow cytometric analysis (Ormerod, 1999) at 24, 48 and 96 h time points. The distribution of cells in different phases of the cell cycle is illustrated in Table 5. Compound **2** at 7  $\mu$ M

Table 1  
Cytotoxic activity of andrographolide **1** and compounds **2–4** against human breast (MCF-7) and colon (HCT-116) cancer cell lines

Compound	GI <sub>50</sub>		TGI		LC <sub>50</sub>	
	MCF-7	HCT-116	MCF-7	HCT-116	MCF-7	HCT-116
<b>1</b>	6.4 ± 2.1	5.1 ± 0.1	64.7 ± 12.2	15.5 ± 9.3	81.1 ± 17.5	39.5 ± 9.1
<b>2</b>	6.7 ± 1.4	3.2 ± 1.6	39.5 ± 15.8	11.2 ± 1.8	66.4 ± 16.2	>100
<b>3</b>	25.5 ± 9.7	13.5 ± 1.1	62.4 ± 9.5	8.9 ± 1.4	55.8 ± 12.9	>100
<b>4</b>	5.9 ± 1.5	5.1 ± 2.3	16.8 ± 9.3	7.6 ± 2.1	82.6 ± 14.6	>100

Values (in  $\mu$ M) are mean of three separate experiments and errors represent the SD values. GI<sub>50</sub>, the molar concentration that produces 50% growth inhibition; TGI, the molar concentration giving total growth inhibition; LC<sub>50</sub>, the molar concentration leading to 50% net cell death.

Table 2  
Cytotoxic activity of compounds **2** (NSC 725619) and **4** (NSC 725620)<sup>a</sup> against NCI human cancer cell line panel

Panel cell lines	Compound					
	<b>2</b>			<b>4</b>		
	GI <sub>50</sub>	TGI	LC <sub>50</sub>	GI <sub>50</sub>	TGI	LC <sub>50</sub>
<i>Leukaemia</i>						
CCRF-CEM	2.08	7.07	>100	1.9	5.62	61.65
K-562	1.90	5.49	>100	1.34	4.67	33.11
MOLT-4	3.16	12.88	>100	1.9	4.46	13.18
RPMI-8226	2.51	6.02	>100	2.19	5.37	>100
SR	2.63	6.16	>100	0.91	3.38	28.84
<i>NSCL cancer</i>						
A549/ATCC	10.71	27.54	69.18	11.48	28.84	70.79
EKVX	25.11	72.44	>100	19.94	40.73	83.17
HOP-62	12.58	26.30	53.7	3.01	11.31	39.81
NCI-H226	4.26	26.91	>100	3.71	30.9	>100
NCI-H322M	20.41	40.73	83.17	18.62	45.7	>100
NCI-H460	20.41	47.86	>100	21.37	48.97	>100
NCI-H522	15.13	51.28	>100	2.95	12.58	>100
<i>Colon cancer</i>						
COLO 205	31.62	100	>100	22.9	50.11	>100
HCC-2998	10.71	24.54	56.23	12.3	26.91	57.44
HCT-116	1.94	4.16	9.12	1.77	4.07	>100
HCT-15	13.18	39.81	>100	1.22	30.9	85.11
HT29	5.37	>100	>100	6.91	27.54	>100
KM12	11.48	36.3	>100	7.24	40.73	>100
SW-620	4.57	69.18	>100	2.88	12.02	>100
<i>CNS cancer</i>						
SF-268	15.48	36.3	83.17	14.12	33.88	79.43
SF-295	16.21	32.35	64.56	8.91	24.54	63.09
SF-539	17.37	77.62	>100	3.63	14.79	72.44
SNB-19	30.19	69.18	>100	19.05	38.9	79.43
SNB-75	18.19	37.15	75.85	16.21	33.11	67.6
U251	10.47	33.11	>100	5.62	24.54	89.12
<i>Melanoma</i>						
LOX IMVI	3.89	17.37	63.09	2.95	12.02	53.7
MALME-3M	20.4	41.68	87.09	13.18	38.01	>100
SK-MEL-2	19.49	50.11	>100	12.08	32.25	85.11
SK-MEL-28	20.41	56.23	>100	15.84	33.11	69.18
SK-MEL-5	15.13	39.81	>100	7.07	22.38	58.88
UACC-257	10.71	24.54	54.95	13.8	28.84	60.22
UACC-62	5.75	21.37	58.88	4.07	17.37	50.11
<i>Ovarian cancer</i>						
IGROV1	17.78	>100	>100	4.46	>100	>100
OVCAR-3	3.16	12.02	42.65	1.44	3.89	12.02
OVCAR-4	23.44	64.56	>100	19.95	35.48	64.56
OVCAR-5	18.62	35.48	66.06	10.47	23.48	52.48
OVCAR-8	2.57	11.74	74.13	9.54	25.7	69.18
SK-OV-3	16.21	41.68	>100	17.78	37.15	77.62
<i>Renal cancer</i>						
ACHN	14.79	33.11	72.44	4.67	18.19	58.88
CAKI-1	13.18	26.91	54.95	0.39	2.75	10.71
SN12C	7.07	23.44	67.6	3.8	22.38	>100
TK-10	20.89	38.01	70.79	14.45	35.48	85.11
UO-31	19.05	39.81	81.28	12.3	28.84	69.18
<i>Prostate cancer</i>						
PC-3	10.96	29.51	77.62	1.86	7.07	35.48
DU-145	16.21	52.48	>100	13.18	30.9	91.2
<i>Breast cancer</i>						
MCF-7	3.71	22.9	>100	5.49	35.48	>100
NCI/ADR-RES	4.07	16.59	70.79	10.71	26.3	64.56

(continued on next page)

Table 2 (continued)

Panel cell lines	Compound					
	<b>2</b>			<b>4</b>		
	GI <sub>50</sub>	TGI	LC <sub>50</sub>	GI <sub>50</sub>	TGI	LC <sub>50</sub>
MDA-MB 231/ATCC	19.05	37.15	72.44	15.13	32.35	69.18
HS 578T	5.07	79.43	>100	9.33	41.68	>100
MDA-MB-435	6.45	22.9	77.62	2.69	8.12	38.01
BT-549	16.59	37.15	70.79	14.45	28.84	57.54
T-47D	22.09	79.43	>100	15.84	44.66	>100
MG_MID	10.23	30.90	79.43	6.45	20.41	64.56

Mean panel values of the response parameter were obtained by averaging the individual values (in  $\mu\text{M}$ ) for each cell line. The activity with respect to dose-response parameters (GI<sub>50</sub>, TGI and LC<sub>50</sub>) and cancer type was not significant between compounds **2** and **4**. The over all GI<sub>50</sub>, TGI and LC<sub>50</sub> of compound **2** was statistically significant ( $p = 0.009$ ,  $p = 0.003$  and  $p = 0.013$ , respectively) compared to compound **4**. MG\_MID, mean graph midpoints.

<sup>a</sup> Data obtained from the NCI's *in vitro* disease-oriented human tumour cells screen (Boyd, 1989; Monks et al., 1991).

Table 3

Mean values of the dose-response parameters (in  $\mu\text{M}$ ) of andrographolide **1**<sup>a</sup>, compounds **2** and **4** in the NCI *in vitro* screen

Dose-response parameters	Compound			<i>p</i> -value		
	<b>1</b>	<b>2</b>	<b>4</b>	<b>1</b> vs <b>2</b>	<b>1</b> vs <b>4</b>	<b>2</b> vs <b>4</b>
GI <sub>50</sub>	16.2	10.2	6.5	<0.001	<0.001	0.009
TGI	49.7	30.9	20.4	<0.001	<0.001	0.003
LC <sub>50</sub>	80.8	79.4	64.6	0.868	0.007	0.013

<sup>a</sup> The values for andrographolide **1** (NSC 383468) are based on previous screens conducted by the NCI where the highest concentration tested was also 100  $\mu\text{M}$ .

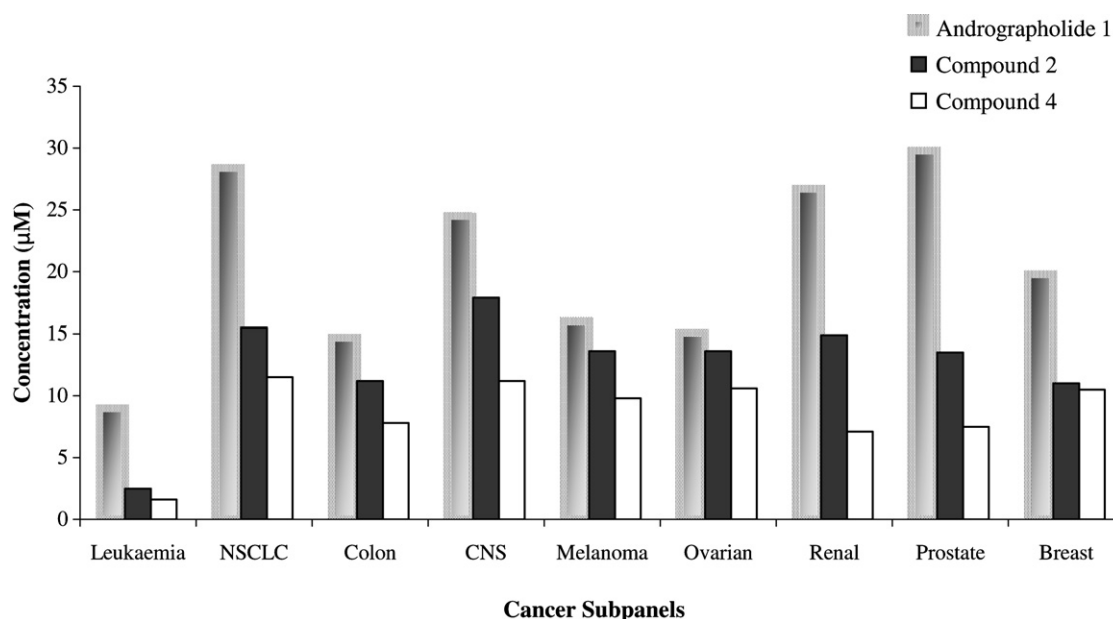


Fig. 2. A panel of 60 human cancer cell lines derived from nine-cancer types were incubated in complete cell growth medium with and without different concentrations of andrographolide **1** or its analogues for 48 h. The percentage growth was determined by sulphorhodamine B method as described under Section 4. Compound **4** was more potent against NSCLC ( $p = 0.001$ ), melanoma ( $p = 0.011$ ) and renal ( $p = 0.022$ ) cancer types compared to that of the parent compound. The activity of the compound **2** was not statistically significant compared with andrographolide **1** except NSCLC ( $p = 0.027$ ) cancer type.

( $\sim\text{GI}_{50}$  value) and 14  $\mu\text{M}$  ( $\sim 2 \times \text{GI}_{50}$  value) concentrations induced G1 phase arrest at the 24 h time point (Table 5). At 48 h with 7  $\mu\text{M}$  concentration, compound **2** induced G1 phase arrest and 14  $\mu\text{M}$  induced a G2/M phase arrest with a decrease in the S phase cells. At 96 h with 7  $\mu\text{M}$  M concentration, compound **2** induced G2/M phase arrest with a

decrease in G1 phase cells, showing a slightly different pattern in its activity compared to that of the parent compound (Srinivasa et al., 2003). Nevertheless, it did not show selectivity towards cells in specific phases of the cell cycle. Compound **4** at 5  $\mu\text{M}$  ( $\sim\text{GI}_{50}$  value) and 10  $\mu\text{M}$  ( $\sim 2 \times \text{GI}_{50}$  value) induced predominantly G2/M phase



Table 4  
COMPARE analysis of compounds **2** and **4** with standard agents (at GI<sub>50</sub> values)

Compound	PCC <sup>a</sup>	Standard agents	Mechanism of action
<b>2</b>	<b>0.673</b>	Hydrazine sulfate	Unknown
	<b>0.614</b>	L-cysteine analogue	Unknown
	0.594	Thioguanine	Antimetabolite
<b>4</b>	0.599	Emolin sodium	Unknown
	0.580	Hydrazine sulfate	Unknown
	0.562	Flavopiridol	CDKs inhibitor

<sup>a</sup> PCC – Pearson correlation coefficient and PCC values >0.6 are considered to indicate a significant similarity to known agents (Weinstein et al., 1997).

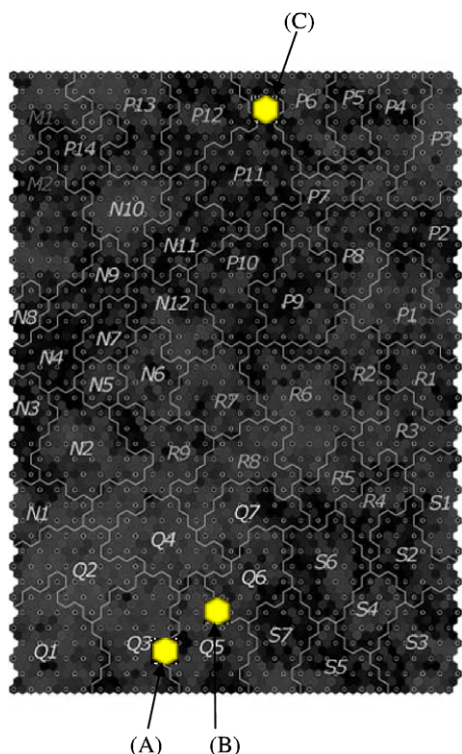


Fig. 3. Location of andrographolide **1** (A), compound **2** (B) and **4** (C) on the SOM map. Based on the cellular activities, SOM cluster analyses has been divided into six major classes: mitosis (M), nucleic acid synthesis (S), membrane transport and integrity (N), phosphatase- and kinase-mediated cell cycle regulation (P), and two remaining regions arbitrarily labelled Q and R could not be assigned to any specific activity class (Covell et al., 2003; Rabow et al., 2002).

arrest in cells treated for 24 and 48 h with reduction in the number of cells in the S phase (Table 5). At 96 h, compound **4** at 5  $\mu$ M induced S phase arrest, which corresponded to a decrease in G1 and G2/M phase cells. These results imply that the mechanism of cell cycle arrest induced by compounds **2** and **4** are different from that of the parent compound (Srinivasa et al., 2003).

### 3. Conclusions

Andrographolide analogues synthesised in this study showed cytotoxic activity against two pre-screen cell lines

and 60 NCI human cancer cell lines. Compounds **2** and **4** showed non-specific phase of the cell cycle arrest in MCF-7 cells treated with different concentrations at different time points. SOM analyses suggested that andrographolide **1** and compound **2** may possess novel mechanism(s) of action and the mode of action of compound **4** might involve targeting phosphatases or kinases that regulates cell cycle. The mechanism(s) of the antitumour activity and further variations of the parent structure are currently being investigated to improve both potency and selectivity and also to obtain more detailed information on the structure activity relationships (SAR).

### 4. Experimental

Solvents (AR grade) for purification of compounds were used as supplied by Fisher Scientific (UK). Silica gel 60 (0.040–0.063 mm) and 20 cm  $\times$  20 cm silica gel 60 F<sub>254</sub>-coated TLC plates were obtained from Merck (Darmstadt, Germany). <sup>1</sup>H and <sup>13</sup>C NMR spectra were recorded on a Bruker ARX 250 instrument, with NMR spectra obtained in deuterated chloroform (CDCl<sub>3</sub>). The chemical shift values  $\delta$  are expressed in parts per million (ppm), with coupling constants (*J*) in Hertz (Hz). Melting points were recorded using an Electrothermal melting point apparatus and are uncorrected. IR spectra (as KBr disks) were measured on a Perkin–Elmer RX I FT-IR spectrometer and frequencies are expressed in cm<sup>–1</sup>. Mass spectra were recorded on a Micromass Platform spectrometer, an AEI MS-902 (nominal mass).

#### 4.1. Synthesis

##### 4.1.1. 3,19-Isopropylideneandrographolide (**2**)

A catalytic amount of pyridinium *p*-toluenesulphonate (few crystals) was added to a solution of benzene solution of benzene/DMSO (34 ml, 7.5:1), andrographolide **1** (1.5 g, 4.3 mmol) and 2,2-dimethoxypropane (2 ml, 16.3 mmol). The reaction mixture was then raised until reflux began. After completion of the reaction within 30 min (monitored by TLC), the contents were cooled to room temperature and basified with Et<sub>3</sub>N (1 ml) in order to quench any remaining catalyst. The mixture was next diluted with benzene (20 ml) and washed with H<sub>2</sub>O (3  $\times$  30 ml). The organic layer was dried (anhydrous Na<sub>2</sub>SO<sub>4</sub>) and concentrated to obtain a yellow coloured solid, which on maceration with Et<sub>2</sub>O gave 3,19-isopropylideneandrographolide (**2**) (1.2 g, 3.1 mmol, 71.8%); m.p. 191–192 °C; IR (KBr) 3482, 2939, 1746, 1223, 1066, 901, 860 cm<sup>–1</sup>; <sup>1</sup>H NMR (250 MHz, CDCl<sub>3</sub>):  $\delta$  6.97 (1H, *td*, *J* = 6.9, 1.4 Hz, H-12), 5.05 (1H, *d*, *J* = 5.7 Hz, H-14), 4.91 (1H, *s*, H-17a), 4.62 (1H, *s*, H-17b), 4.46 (1H, *dd*, *J* = 10.4, 5.9 Hz, H-15a), 4.27 (1H, *dd*, *J* = 10.4, 1.9 Hz, H-15b), 3.97 (1H, *d*, *J* = 11.6 Hz, H-19a), 3.52 (1H, *s*, H-3), 3.18 (1H, *d*, *J* = 11.6 Hz, H-19b), 2.57 (2H, *t*, *J* = 6.8 Hz, H-11), 1.42 (3H, *s*, CH<sub>3</sub>), 1.37 (3H, *s*, CH<sub>3</sub>), 1.20 (3H, *s*, H-18), 0.97 (3H, *s*, H-20); <sup>13</sup>C

Table 5  
Effect of compounds **2** and **4** on cell cycle phase distribution of MCF-7 cells

Compound	Concentration ( $\mu\text{M}$ )	24 h			48 h			96 h		
		G1	S	G2/M	G1	S	G2/M	G1	S	G2/M
Control	0	40.6	40.3	22.0	42.2	40.8	16.8	47.2	38.5	14.2
<b>2</b>	7	<b>52.1</b>	24.2	23.6	<b>52.8</b>	33.1	13.3	38.8	39.2	<b>21.9</b>
	14	<b>64.1</b>	19.5	16.3	41.6	36.4	<b>21.9</b>		ND	
<b>4</b>	5	41.2	28.4	<b>31.7</b>	45.0	34.2	<b>20.6</b>	33.5	<b>56.1</b>	10.3
	10	42.2	28.2	<b>28.8</b>	33.3	37.1	<b>29.4</b>		ND	

Cell cycle phase distribution of MCF-7 cells (expressed in %) after 24 h, 48 h and 96 h exposure to compounds **2** and **4**. Values are the mean of two experiments and the average difference is <10% of the mean value. Numbers in bold correspond to the significant variations compared to control. ND: not determined.

NMR (250 MHz,  $\text{CDCl}_3$ ):  $\delta$  170.4, 149.4, 147.4, 18.7, 128.4, 109.3, 99.5, 74.7, 66.6, 64.3, 56.5, 27.4, 23.6, 16.6; EIMS  $m/z$ : 390  $[\text{M}^+]$ .

#### 4.1.2. 14-Acetyl-3,19-isopropylideneandrographolide (**3**) and 14-acetylandrographolide (**4**)

A solution of compound **2** (0.7 g, 2.0 mmol) and  $\text{Ac}_2\text{O}$  (5.2 ml, 55.1 mmol) were heated until reflux began. After completion of the reaction within 45 min (monitored by TLC), the contents were cooled to room temperature, diluted with  $\text{H}_2\text{O}$  (30 ml) and extracted with  $\text{CH}_2\text{Cl}_2$  ( $3 \times 10$  ml). The organic layer was separated, dried (anhydrous  $\text{Na}_2\text{SO}_4$ ) and concentrated. The reaction product was purified by silica gel CC (hexane: $\text{EtOAc}$  = 85:15) to obtain the colourless products 14-acetyl-3,19-isopropylideneandrographolide (**3**) (0.26 g, 0.6 mmol, 30.1%), and 14-acetylandrographolide (**4**) (0.32 g, 0.8 mmol, 40.8%), with the latter being crystallized from MeOH.

#### 4.1.3. 14-Acetyl-3,19-isopropylideneandrographolide (**3**)

Crystallised from  $\text{CH}_2\text{Cl}_2$  and MeOH (1:1); m.p. 193–194 °C; IR (KBr) 3434, 2939, 1751, 1231, 1023, 892  $\text{cm}^{-1}$ ;  $^1\text{H}$  NMR (250 MHz,  $\text{CDCl}_3$ ):  $\delta$  7.03 (1H, *td*,  $J$  = 6.9, 1.7 Hz, H-12), 5.93 (H, *d*,  $J$  = 6.0 Hz, H-14), 4.90 (1H, *s*, H-17a), 4.24 (1H, *dd*,  $J$  = 11.2, 1.9 Hz, H-15a), 3.96 (1H, *d*,  $J$  = 11.2 Hz, H-15b), 3.50 (1H, *dd*,  $J$  = 8.4, 3.7 Hz, H-3), 3.18 (1H, *d*,  $J$  = 11.5 Hz, H-19b), 2.12 (3H, *s*), 1.45 (3H, *s*), 1.36 (3H, *s*), 1.20 (3H, *s*, H-18), 0.94 (3H, *s*, H-20);  $^{13}\text{C}$  NMR (250 MHz,  $\text{CDCl}_3$ ):  $\delta$  169.5, 168.0, 122.8, 107.8, 98.2, 70.6, 66.8, 25.9, 23.2, 19.6, 15.1; EIMS  $m/z$ : 432  $[\text{M}^+]$ .

#### 4.1.4. 14-Acetylandrographolide (**4**)

m.p. 169–170 °C; IR (KBr) 3415, 2939, 1747, 1226, 1022, 893  $\text{cm}^{-1}$ ;  $^1\text{H}$  NMR (250 MHz,  $\text{CDCl}_3$ ):  $\delta$  7.01 (1H, *td*,  $J$  = 6.8, 1.5 Hz, H-12), 5.92 (1H, *d*,  $J$  = 6.0 Hz, H-14), 4.88 (1H, *s*, H-17a), 4.26 (1H, *dd*,  $J$  = 10.6, 1.8 Hz, H-15a), 3.48 (1H, *t*,  $J$  = 7.9 Hz, H-3), 3.32 (1H, *d*,  $J$  = 10.6 Hz, H-15b), 2.87 (2H, *bs*), 2.12 (3H, *s*, OAc), 1.25 (3H, *s*, H-18), 0.67 (3H, *s*, H-20);  $^{13}\text{C}$  NMR (250 MHz,  $\text{CDCl}_3$ ):  $\delta$  170.8, 169.4, 150.8, 147.1, 124.3, 109.1, 71.9, 68.2, 55.6, 28.6, 23.1, 15.9; EIMS  $m/z$ : 374  $[\text{M}^+ - \text{H}_2\text{O}]$ .

#### 4.2. Cell culture

For routine testing, two cancer cell lines were used in this study as a pre-screen: MCF-7 and HCT-116 cancer cell lines were purchased from American Type Cell Collection (ATCC), Rockville, MD, USA. Cells were cultured in RPMI 1640 medium with L-glutamine, supplemented with 10% heat inactivated (55 °C for 1 h) foetal bovine serum (FBS), 200 U/ml of penicillin and 200  $\mu\text{g}/\text{ml}$  of streptomycin, at 37 °C in an atmosphere of 5%  $\text{CO}_2$  and 95% air.

#### 4.3. MTT cell viability assay

MTT assay was carried out based on the method described by Mosmann (1983). Briefly, cells were plated in 96-well flat bottom tissue culture plates at initial seeding densities between 3000 and 5000 cells per well in a volume of 180  $\mu\text{l}$  of culture media. Cells were incubated at 37 °C (5%  $\text{CO}_2$  and 95% air) overnight to allow attachment on to the wells. Drugs were diluted serially ranging from 0.01  $\mu\text{M}$  to 1000  $\mu\text{M}$  and 20  $\mu\text{l}$  of each drug dilution was added into the appropriate wells in four replicates. Following incubation at 37 °C in an atmosphere of 5%  $\text{CO}_2$  and 95% air for 72 h, 50  $\mu\text{l}$  of MTT (2 mg/ml in PBS) was added into each well containing the cells in 200  $\mu\text{l}$  medium. The plates were re-incubated for 4 h to allow metabolism of MTT by cellular mitochondrial dehydrogenases after which the supernatant was aspirated. The formazan crystals formed were dissolved by the addition of 150  $\mu\text{l}$  of DMSO:glycine buffer (4:1) (0.1 M glycine/0.1 M NaCl/pH 10.5). The plates were shaken and the absorbance of formazan was read at 550 nm on an Anthos microplate reader (Anthos Labtec Instruments GmbH, Lagerhausstr, Austria). The absorbance of the purple formazan at 550 nm is proportional to the number of viable cells. For both the cell lines, zero-day cell densities (by MTT end point) were also determined in order to obtain percentage growth of cells post-treatment. The results were analysed using Deltasoft 3 computer program (BioMetallics Inc., Princeton, NJ, USA). From the semi-log dose–response curves (percentage of growth vs concentration), three dose–response parameters ( $\text{GI}_{50}$ , TGI and  $\text{LC}_{50}$ ) were determined.

#### 4.4. NCI *in vitro* screen

Sulforhodamine B assay was used for assessing the cytotoxicity of test agents in a panel of 60 cell lines (Boyd and Paull, 1995). Briefly, the human cancer cell lines of the cancer screening panel were grown in RPMI 1640 medium containing 5% FBS and 2 mM L-glutamine. For a typical screening experiment, cells were inoculated into 96-well microtiter plates in 100  $\mu$ l of medium at plating densities depending on the growth characteristics of specific cell lines. After cell inoculation, the microtiter plates were incubated at 37 °C, 5% CO<sub>2</sub>, 95% air and 100% relative humidity for 24 h prior to addition of experimental drugs. Following drug addition, the plates were incubated for 48 h and change in protein stain optical density allowed the inhibition of cell growth to be analysed.

#### 4.5. NCI's COMPARE and SOM cluster analyses

The NCI COMPARE analysis was used to identify the probable mechanistic categories of compounds tested in the NCI cell lines. COMPARE analysis utilises the *in vitro* antitumour results in determining and expressing the degree of similarity, or lack thereof, of mean-graph profiles generated on a similar compound or different compounds (Weinstein et al., 1997). COMPARE searches the standard anticancer agent database (171 in total) for those similar to a novel compound and SAS (Statistical Analysis System) statistical program was used to determine the Pearson Correlation Coefficient (PCC) values. Similarity in the pattern of activity often indicates similarity in mechanism of action, mode of resistance and molecular structure (Osdol et al., 1994).

The SOM cluster analyses introduced in 1997 represents an alternative to the more classical COMPARE analysis and identifies relationships between chemotypes of screened agents and their effect on six major classes of cellular activities: mitosis (M), nucleic acid synthesis (S), membrane transport and integrity (N), phosphatase- and kinase-mediated cell cycle regulation (P), and two remaining regions arbitrarily labelled Q and R could not be assigned to any specific activity class (Covell et al., 2003; Rabow et al., 2002).

#### 4.6. Cell cycle analysis by flow cytometry

MCF-7 cells were plated in six-well plates (Nalgene-Nunc) containing  $5 \times 10^6$  cells per well in 3 ml medium and were left to attach overnight at 37 °C (5% CO<sub>2</sub> and 95% air) before treatment with compounds of different concentrations. Followed by incubation of treated cells for the duration of the experiment, the attached cells were trypsinised, washed twice in PBS, and incubated in 0.5 ml fluorochrome solution (contents) for overnight in the dark at 4 °C. The DNA contents (PI bound to DNA) of 20,000 cells were analysed by flow cytometry (EPICS, Beckman

Coulter) in which an argon laser (488 nm) was used to excite PI and emission above 550 nm was collected. Data analysis of PI content histograms was carried out by gating the histograms in Expo\_32 or using the computer advanced DNA cell cycle analysis software Multicycle for Windows (Phoenix Flow Systems, San Diego, California).

#### 4.7. Statistical analysis

Statistical comparisons were made using *t*-test, one-way ANOVA and Tukey tests (Steel and Torrie, 1985) of multiple comparisons by statistical package for social sciences (SPSS) version 12.00. A level of significance of  $p < 0.05$  was utilised and the results were expressed as the arithmetic mean and standard deviation (SD).

#### Acknowledgements

The Malaysian Ministry of Science, Technology and Innovation (MOSTI) is thanked for funding this project under the Intensification of Research in Priority Areas (IRPA) Programme (Grants: 06-02-04-0088 and 06-02-04-0603-EA001). The authors thank National Cancer Institute (NCI, USA) for *in vitro* pharmacological screening. We thank Dr. Andrew McCarroll, the University of Nottingham, UK for spectroscopic interpretation and help in this study.

#### References

- Amroyan, E., Gabrielian, E., Panossian, A., Wikman, G., Wagner, H., 1999. Inhibitory effect of andrographolide from *Andrographis paniculata* on PAF-induced platelet aggregation. *Phytomedicine* 10, 47–60.
- Basak, A., Cooper, S., Andree, G.R., Banik, U.K., Michel, C., Nabil, G.S., 1999. Inhibition of proprotein convertases-1, -7 and furin by diterpenes of *Andrographis paniculata* and their succinoyl esters. *Biochem. J.* 338, 107–118.
- Boyd, M.R., 1989. Status of the NCI preclinical antitumour drug discovery screen: implications for selection of new agents for clinical trials. In: DeVita, V.T., Hellman, S., Rosenberg, S. (Eds.), *Cancer: Principles and Practice of Oncology Updates*, vol. 3. Lippincott, Philadelphia, pp. 1–12.
- Boyd, M.R., Paull, K.D., 1995. Some practical considerations and applications of the national cancer institute *in vitro* anticancer drug discovery screen. *Drug Develop. Res.* 34, 91–109.
- Chang, H.M., But, P.P.-H., 1987. In: Yeung, S.S., Yao, S.C., Wang, L.L. (Eds.), *Pharmacology and Applications of Chinese Materia Medica*, vol 2. World Scientific, Singapore, pp. 918–928.
- Chopra, R.N., Nayar, S.L., Chopra, I.C., 1956. *Glossary of Indian Medicinal Plants*. Council for Scientific and Industrial Research, New Delhi.
- Covell, G.D., Anders, W., Alfred, A.R., Narmada, T., 2003. Molecular classification of cancer: unsupervised self-organizing map analysis of gene expression microarray data. *Mol. Cancer Ther.* 2, 317–332.
- Fujita, T., Fujitani, R., Takeda, Y., Takaishi, Y., Yamada, T., Kido, M., Miura, I., 1984. On the diterpenoids of *Andrographis paniculata* X-ray crystallographic analysis of andrographolide and structure determination of new minor diterpenoids. *Chem. Pharm. Bull.* 32, 2117–2125.



- Handa, S.S., Sharma, A., 1990. Hepatoprotective activity of andrographolide against galactosamine and paracetamol intoxication in rats. *Indian J. Med. Res.* 92, 284–292.
- Kapil, A., Koul, I.B., Banerjee, S.K., Gupta, B.D., 1993. Antihepatotoxic effects of major diterpenoid constituents of *Andrographis paniculata*. *Biochem. Pharmacol.* 46, 182–185.
- Kleipool, R.J.C., 1952. Constituents of *Andrographis paniculata*. *Nature* 169, 33–34.
- Matsuda, T., Kuroyangagi, M., Suguyama, S., Umehara, K., Ueno, A., Nishi, K., 1994. Cell differentiation-inducing diterpenes from *Andrographis paniculata* Nees. *Chem. Pharm. Bull.* 42, 1216–1225.
- Monks, A., Scudiero, D., Skehan, P., Shoemaker, R., Paull, K., Vistica, D., Hose, C., Langley, J., Cronise, P., Vaigro-Wolff, A., 1991. Feasibility of a high flux anticancer drug screen using a diverse panel of cultured human tumour cell lines. *J. Natl. Cancer Inst.* 83, 757–766.
- Mosmann, T., 1983. Rapid colorimetric assay for cellular growth and survival: application to proliferation and cytotoxicity assays. *J. Immunol. Meth.* 65, 55–63.
- Nanduri, S., Nyavanadi, V.K., Thunuguntla, S.S.R., Kasu, S., Pallerla, M.K., Ram, P.S., Rajagopal, S., Kumar, R.A., Ramanujam, R., Babu, J.M., Vyas, K., Devi, A.S., Reddy, G.O., Akella, V., 2004. Synthesis and structure-activity relationships of andrographolide analogues as novel cytotoxic agents. *Bioorg. Med. Chem. Lett.* 14, 4711–4717.
- Ormerod, M.G., 1999. *Flow Cytometry: A Practical Approach*, second ed. IRL Press, Oxford, New York.
- Osdol, V., Myers, T.G., Paull, K.D., Kohn, K.W., Weinstein, J.N., 1994. Use of the Kohonen self-organizing map to study the mechanisms of action of chemotherapeutic agents. *J. Natl. Cancer Inst.* 86, 1853–1859.
- Puri, A., Saxena, R., Saxena, R.P., Saxena, K.C., 1993. Immunostimulant agents from *Andrographis paniculata*. *J. Nat. Prod.* 56, 995–999.
- Rabow, A.A., Shoemaker, R.H., Sausville, E.A., Covell, D.G., 2002. Mining the National Cancer Institute's tumour-screening database: identification of compounds with similar cellular activities. *J. Med. Chem.* 45, 818–840.
- Rajagopal, S., Ajaya, K.R., Devi, D.S., Satyanarayana, C., Rajagopalan, R., 2003. Andrographolide, a potential cancer therapeutic agent isolated from *Andrographis paniculata*. *J. Expt. Ther. Onc.* 3, 147–158.
- Satyanarayana, C., Deevi, D.S., Rajagopalan, R., Srinivas, N., Rajagopal, S., 2004. DRF 3188 a novel semi-synthetic analogue of andrographolide: cellular response to MCF-7 breast cancer cells. *BMC Cancer* 4, 1–8.
- Senderowicz, A.M., Headlee, D., Stinson, S.F., Lush, R.M., Kalil, N., Villalba, L., Hill, K., Steinberg, S.M., Figg, W.D., Tompkins, A., 1998. Phase I trial of continuous infusion flavopiridol, a novel cyclin-dependent kinase inhibitor, in patients with refractory neoplasm. *J. Clin. Oncol.* 16, 2986–2999.
- Smith, A.B., Toder, B.H., Carroll, P.J., Donohue, J., 1982. Andrographolide: an X-ray crystallographic analysis. *J. Crystallogr. Spectrosc. Res.* 12, 309–319.
- Siripong, P., Konckathip, B., Preechanukool, K., Picha, P., Tunsuwan, K., Taylor, W.C., 1992. Cytotoxic diterpenoid constituents from *Andrographis paniculata* Nees leaves. *J. Sci. Soc. Thai* 18, 187–194.
- Spek, A.L., Duisenberg, A.J.M., Labadie, R.P., Ratnayake, S., Abeysekera, A., De Silva, K.T.D., 1987. Hydrogen bonding in andrographolide: 3-[2-[decahydro-6-hydroxy-5-(hydroxymethyl)-5,8a-dimethyl-2-methylene-1-naphthalenyl] ethylidene] dihydro-4-hydroxy-2(3H)-furanone. *Acta Crystallogr.* C43, 530–532.
- Srinivasa, R.J., Stanlas, J., Lajis, N.H., Said, S., Hamzah, A.S., McCarroll, A., Matthews, C., Stevens, M.F.G., 2003. APAG-1 derivatives as antitumour agents. *Brit. J. Cancer* 88 (Suppl. 1), S25–S54.
- Srinivasa, R.J., McMillan, K., Carl, H., Hamzah, A.S., Saad, M.S., Lajis, N.H., Stevens, M.F.G., Stanlas, J., 2006a. 14-Acetylandrographolide. *J. Chem. Crystallogr.* 36, 93–97.
- Srinivasa, R.J., Hamzah, A.S., Saad, M.S., Lajis, N.H., Stevens, M.F.G., Stanlas, J., 2006b. Semisynthesis and cytotoxic activities of andrographolide analogues. *J. Enzym. Inhib. Med. Ch* 21, 145–155.
- Stanlas, J., Liew, P.S., Iftikhar, N., Lee, C.P., Saad, S., Lajis, N., Robins, R.A., Loadman, P., Bibby, M.C., 2001. APAG-1 as antitumour agent. *Eur. J. Cancer* 37, 169.
- Steel, R.G.D., Torrie, H.J., 1985. In: *Bioestadística, Principios y procedimientos*. McGraw-Hill, Bogota, pp. 322–340.
- Visen, P.K., Shukla, B., Patnaik, G.K., Dhawan, B.N., 1993. Andrographolide protects rat hepatocytes against paracetamol-induced damage. *J. Ethnopharmacol.* 40, 131–136.
- Weinstein, J.N., Mayers, T.G., O'Conner, P.M., Friend, S.H., Forance, A.J., Kohn, K.W., Fojo, T., Bates, S.E., Rubinstein, L.V., Anderson, N.L., Buolamwin, J.K., Osdol, V., Monks, P., Scudiero, D.A., Sausville, E.A., Zaharevitz, D.W., Bunow, B., Viswahanadan, V.N., Wittes, R.E., Paull, K.D., 1997. An information-intensive approach to the molecular pharmacology of cancer. *Science* 275, 343.
- Zhang, X.F., Tan, B.K., 2000. Antihyperglycaemic and anti-oxidant properties of *Andrographis paniculata* in normal and diabetic rats. *Clin. Exp. Pharmacol. Physiol.* 27, 358–363.